SPE-185805-MS

Development of a Parallel Simulator Utilizing Multiple Interacting Continua and Embedded Discrete Fracture Models in Fractured Unconventional Reservoirs

Kun Wang, Hui Liu, Jia Luo, and Zhangxin Chen, Department of Chemical and Petroleum Engineering, University of Calgary

This paper was prepared for presentation at the SPE Europec featured at 79th EAGE Conference and Exhibition held in Paris, France, 12–15 June 2017.

Abstract

Unconventional petroleum reservoirs, such as shale gas and tight oil reservoirs, have changed the entire energy equation in the world. An accurate and efficient reservoir simulator is essential for the development and management of these reservoirs and the optimization of their production schedules. However, the gas storage and transport mechanisms in ultra-tight matrix, including gas adsorption/desorption, non-Darcy flow, and surface diffusion, are different from those in conventional petroleum reservoirs. In addition, hydraulic fracturing techniques are often required to achieve their economical production, which leads to existence of complex fracture networks in the unconventional reservoirs. These features of unconventional reservoirs make their accurate numerical simulations a big challenge. In this paper, we develop a simulator for fractured unconventional reservoirs, which takes the specific gas storage and transport mechanisms into consideration, employs a multiple interacting continua (MINC) model to handle well connected natural fractures, utilizes an embedded discrete fracture model to simulate large-scale disconnected hydraulic fractures, and uses a coupled model to efficiently describe multi-scale fractures with irregular geometries. To reduce the computational time, parallel computing techniques are also employed, with which large-scale reservoir simulation cases can be finished in practical time. From the numerical experiments, we can see that reasonable physical phenomena is captured and accurate predictions are performed by this simulator.

Introduction

Unconventional petroleum reservoirs, such as shale gas and tight oil reservoirs, have gradually become one of the key resources in energy supply in the world. In the development and exploration of an unconventional reservoir, an accurate and efficient numerical simulation plays an important role. However, the features of unconventional reservoirs bring tremendous difficulties to the establishment and implementation of mathematical models that are capable of accurately describing these specific features.

It is generally agreed that gas stores as free gas and adsorbed gas on surfaces of organic matters in the shale matrix. It is reported that the adsorbed gas is around 20%-85% of the total gas in place [13]. The adsorbed gas may make a huge contribution to the gas production. Thus the gas adsorption must not be

neglected in unconventional reservoirs. The average size of nanopores, shown by the laboratory results, is usually between 1 and 100 nanometers, which does not satisfy the assumption of the conventional Darcy's law. To describe the gas flow in nanopores, the Knudsen number, which is the ratio of the average free path of gas to a matrix nanopore diameter, is introduced to classify the flow types [35]. Typically, there are four types of flow, which are Knudsen diffusion, transition flow, slippage flow and continuum flow depending on the value of the Knudsen number. Apparent permeability is usually employed as a unified form to represent the non-Darcy flow mechanisms. In fractured reservoirs, geomechanics effects are significant and must be taken into account by numerical simulation since the permeability is very sensitive to a stress change. Without geomechanics effects, the closure of fractures and a reduction in fracture permeability cannot be captured and well production is over-estimated.

To achieve economical production, hydraulic fracturing techniques are the common engineering methods. Large-scale hydraulic fractures generated by hydraulic fracturing connect with pre-existing natural fractures and form complex fracture networks. Multiple continua methods and discrete fracture methods are two of the most widely used methods to describe fractured reservoirs. A dualporosity model proposed in [34] is the first multiple-continuum type method, which divides each grid block into two sub-blocks. The inner one is to represent a matrix block, while the outer one is for fractures. Instead of two sub-blocks, a series of nested sub-blocks are used by a multiple interacting continua method [27, 36] to capture the potential gradients in the tight matrix. The assumption in multiple continua methods that fractures are distributed uniformly and well connected is not satisfied in hydraulic fractures. It is natural to use a discrete fracture model to describe hydraulic fractures with an unstructured grid and calculate the fluid flow in a lower dimension. In order to avoid the difficulty of the generation of unstructured grids, an embedded discrete fracture model is developed by Li et al. [19]. For an embedded discrete fracture model, a structured grid is used to describe the matrix, while fractures are divided into segments and represented by an additional grid. The fluids in the matrix and fractures are coupled with a mass transfer term. However, it is not practical to describe all the fractures with different scales with an embedded discrete fracture model due to its expensive computational cost. Jiang et al. [18, 16] coupled a multiple interacting continua model with an embedded discrete fracture model. In their method, natural (small-scale) fractures are represented by a multiple interacting continua model, and hydraulic (large-scale) fractures are represented by an embedded discrete fracture model. In [37], Zhang et al. coupled a dual-porosity dual-permeability model with a discrete fracture model on unstructured grids. Jiang et al. and Zhang et al. both assumed that hydraulic fractures only connect with natural fractures and a fluid cannot directly flow from the matrix to the hydraulic fractures.

To efficiently and accurately simulate the fluid behavoir in a porous medium, researchers have made significant efforts in the development of simulators and fast numerical methods. Linear solvers are extremely important for reservoir simulation, and more than half of the total simulation time is spent on the solution of linear systems when a reservoir has a number of grid blocks of order 100,000 [9]. The ILU (incomplete LU factorization) [30, 2] preconditioned Krylov subspace methods [28] are usually employed by commercial software as a default linear solver. In [29, 3], the constrained pressure residual (CPR) method was developed to improve the efficiency of a linear system solution process. Based on similar ideas, the FASP (fast auxiliary space preconditioning) method [14] and a family of CPR-type preconditioners [22, 32, 23] were developed. For simulators, Dogru et al. [11, 12] developed a parallel simulator and successfully applied this simulator to billion grid block cases; Li et al. [20] developed a multi-continuum multiple flow mechanism simulator for unconventional oil and gas reservoirs; in [32, 33], a parallel simulator supporting black oil and compositional models was developed for large-scale conventional and unconventional reservoir simulations.

Mathematical Model

In this paper, the black oil model is employed to simulate the multi-phase flow behavior in a porous medium, which can be written as [7, 6, 8]

$$\begin{cases} \dfrac{\partial(\phi s_o \rho_o)}{\partial t} + \nabla \cdot (\dfrac{\mathbf{K} K_{ro} \rho_o}{\mu_o} \nabla \Phi_o) = q^o \quad \text{for the oil component,} \\ \dfrac{\partial(\phi s_w \rho_w)}{\partial t} + \nabla \cdot (\dfrac{\mathbf{K} K_{rw} \rho_w}{\mu_w} \nabla \Phi_w) = q^w \quad \text{for the water component,} \\ \dfrac{\partial(\phi s_g \rho_g + \phi s_o \rho_o R_s)}{\partial t} + \nabla \cdot (\dfrac{\mathbf{K} K_{rg} \rho_g}{\mu_g} \nabla \Phi_g) + \nabla \cdot (\dfrac{\mathbf{K} K_{ro} R_s \rho_o}{\mu_o} \nabla \Phi_o) = q^g + q^o R_s \quad \text{for the gas component.} \end{cases} \tag{1}$$

For unconventional reservoirs, generally, the ultra-tight shale matrix consists of organic and inorganic matters. The pores in organic matters are usually from nanoscale (approximately 2 nanometers) to micro-scale (from 2 to 50 nanometers). The gas storage and fluid transport mechanisms in ultra-tight matrix differ from those in conventional reservoirs. Another important feature we should consider is that the permeability of fractures is sensitive to a stress change. The depletion of pressure occurring during production leads to a dramatic change in fluid conductivity. Hence, the above equations must be modified according to these features of unconventional reservoirs.

Javadpour [15] stated that both free gas and adsorbed gas stores in organic matters. In [13], Hill and Nelson reported that 20%-85% of the total gas is stored as adsorbed gas. Hence, gas adsorption becomes an important mechanism and makes a significant contribution to gas production, which should be taken into consideration. The quantity of adsorbed gas on surfaces of organic matters is usually estimated by

$$m_g = (1-\phi)\rho_r \alpha_g \rho_g V_E, \tag{2}$$

where ρ_r is the density of organic matters (lbm/ft^3); ρ_g is the gas density (lbm/ft^3); α_g is the adsorbed gas density to free gas density ratio; and V_E is the adsorption isotherm function (ft^3/lbm). In [1], α_g was reported as 1.8-2.5. The adsorption isotherm function can be expressed by

$$V_E = V_L \frac{p_g}{p_g + p_L}, \tag{3}$$

where V_L is the Langmuir volume (ft^3/lbm); p_L is the Langmuir pressure (psia). If real gas is considered, Eqn. (3) can be written as

$$V_E = V_L \frac{\frac{p_g}{Z}}{\frac{p_g}{Z} + p_L}, \tag{4}$$

where Z is the compressibility factor. In [31], for some shale samples, the adsorption function obeys the BET isotherm. The general form of the BET isotherm is

$$V_E = \frac{V_L^{\mathrm{BET}} C p_g}{(p_g - p_s)(1 + (C-1)\frac{p_g}{p_s})}, \tag{5}$$

where V_L^{BET} is the BET maximum adsorption capacity at a given temperature, ft^3/lbm; C is the BET equilibrium constant that controls the sorption-isotherm behavior at lower pressure values; p_s is the saturation pressure of the gas, psia.

For the formations of unconventional reservoirs, an apparent permeability correlation is included in our simulator to describe various non-Darcy flow mechanisms in a general form. The apparent permeability of matrix is represented by

$$K_a = K_i \cdot F(K_n), \tag{6}$$

where K_i is the intrinsic permeability of matrix at the initial condition, K_n is the Knudsen number, and $F(K_n)$ is a correction factor. The correction factor is

$$F(K_n) = (1 + \alpha K_n)(1 + \frac{4K_n}{1+K_n}), \tag{7}$$

and α is the rarefaction parameter

$$\alpha = \frac{128}{15\pi^2}\tan^{-1}(4K_n^{0.4}). \tag{8}$$

The Knudsen number K_n is defined by the ratio of the mean free path of gas at reservoir conditions and a hydraulic radius. The Knudsen number K_n can be used to classify the gas flow into continuum flow, slippage flow and transition flow; see Fig. 1.

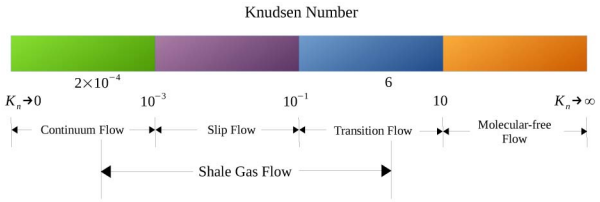

Figure 1—Shale gas transport regimes in nanopores

The permeability change of fractures is usually related to mean normal stress. To simplify the calculation of a permeability change, Chen et al. [4] developed a model for natural fractures, which can be expressed as

$$K = K_i e^{c\frac{1+v}{1-v}\alpha_B(p_g - p_g^0)}, \tag{9}$$

where K_i is the initial permeability (D), c is compressibility (1/psia), v is Poisson's ratio, and α_B is a Biot coefficient. In our simulator, Eqn. (9) is employed to calculate the permeability of matrix, and natural and hydraulic fractures. Normally, the permeability of matrix is not very sensitive to a stress change. The permeability of natural fractures is more sensitive to the stress change than that of hydraulic fractures due to the existence of proppants.

A MINC Model for Ultra-tight Matrix and Well Connected Fractures

A multiple interacting continua model was first proposed in [27, 36], which can be seen as an enhancement of a dual-porosity model [34]. A MINC model employs a series of nested media to capture the large potential gradients inside the matrix, especially in the ultra-tight shale matrix. More importantly, the organic and inorganic matters can be represented by the nested media in a more realistic way, and different gas storage and transport mechanisms can be naturally treated. In Fig. 2, the yellow color outlines the organic matter and the red color represents the pores. We can see that the volume of organic matter is very small and surrounded by inorganic material, thus the inner sub-blocks are used to represent the organic matter and the outer sub-blocks are for the inorganic matter. According to the assumption in a MINC model, the fractures represented by the MINC model should be distributed uniformly and are well connected in the rock matrix. Since the distribution of natural fractures is often random and difficult to get through a micro-seismic method, it is reasonable to represent the natural fractures by the outermost sub-blocks in the MINC model. Fig. 3 illustrates the MINC model for ultra-tight matrix and well connected natural fractures.

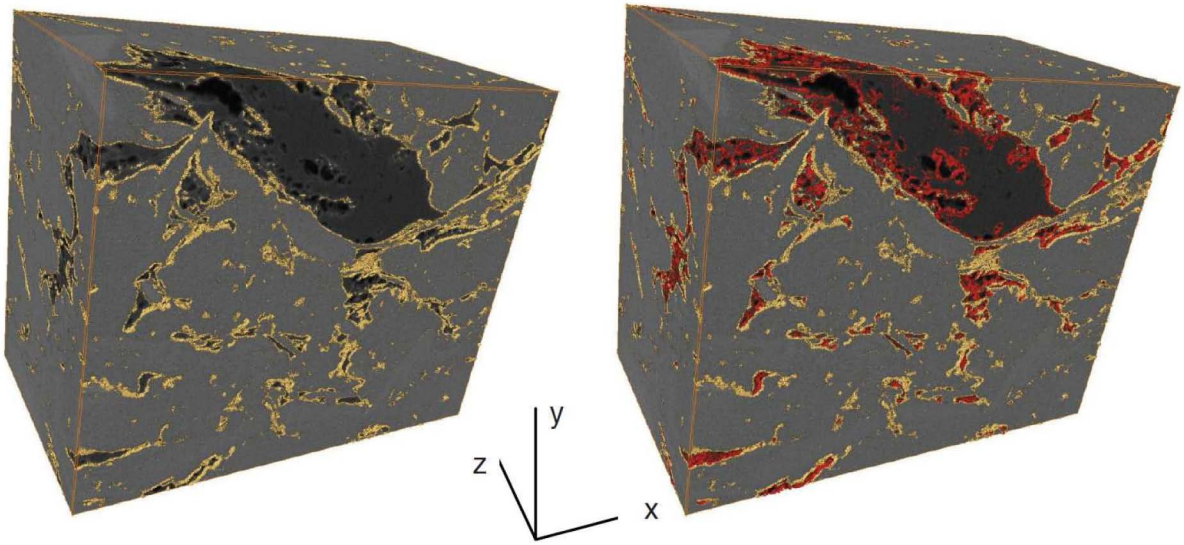

Figure 2—3D FIG/SEG segmentations of 300 separate 2D SEG scans: sample size is 4/m high, 4 /m and 2.5 /m [1]

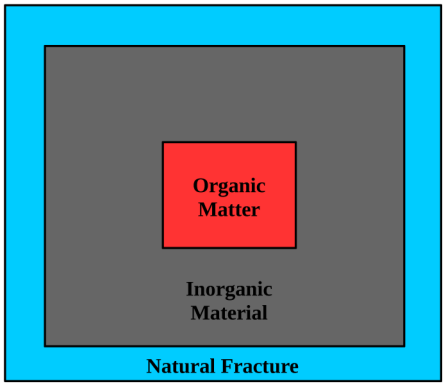

Figure 3—The MINC model for ultra-tight matrix and well-connected natural fractures

An Embedded Discrete Fracture Model in Disconnected Large-scale Fractures

The assumption in a MINC model is not satisfied for disconnected large-scale fractures, such as hydraulic fractures. Consequently, a MINC model is not adequate to model hydraulic fractures. Discrete fracture models employ unstructured grids to describe fractures, simulate the fluid flow in a lower dimension and couple the fluid flow in fractures and in the matrix via proper boundary conditions. In [19], Li et al. proposed an embedded discrete fracture model (EDFM), which uses structured grids for the matrix, introduces an additional grid to represent hydraulic fractures, and couples the fluid flow between matrix and fractures through a mass transfer term. An embedded discrete fracture model is capable of avoiding the difficulty of generation of unstructured grids. In an embedded discrete fracture model, the transmissibility of four types of connections should be calculated. The first type of connection is between matrix and hydraulic fractures represented by the EDFM; the second type of connection is between two intersecting fractures represented by the EDFM; the third type of connection is between two fracture cells of an individual fracture represented by the EDFM; and the fourth type is between the natural fractures represented by the MINC model and the hydraulic fractures represented by the EDFM. Details of transmissibility calculation can be seen in [19, 26].

A Coupled Model for Multi-scale Complex Fracture Networks

In [18, 16, 17], Jiang et al. described hydraulic and small fractures by coupling the EDFM and multi-continuum approaches for unconventional gas reservoirs. They assumed that hydraulic fractures only connect with natural fractures, which means that it is only possible for the fluid to flow from the matrix to natural fractures first and then from the natural fractures to the hydraulic fractures. This assumption is reasonable when the permeability of natural fractures is much larger than that of the matrix. However, the permeability of natural fractures is very sensitive to a stress change. During production, the reservoir pressure drops, which leads to the closure of natural fractures and consequently a dramatic reduction in permeability. In order to accurately predict the production of unconventional reservoirs with multi-scale fractures, a new coupled model is developed.

To explain the model, we take the grid shown in Fig. 4a as an example. Four grid blocks C_i, i = 1,2,3,4 and one hydraulic fracture is contained in the grid. The hydraulic fracture passes through three blocks, C_1, C_2 and C_4. We divide each grid block into three sub-blocks, use the most inner sub-blocks, $m_{i,2}$, i = 1,2,3,4, to represent organic matters, utilize the sub-blocks, $m_{i,1}$, i = 1,2,3,4 to represent inorganic matters, and employ the most outer sub-blocks, f_i, i = 1,2,3,4, to represent the natural fractures. The hydraulic fracture is divided into three segments by the grid blocks, which are F_i, i = 1,2,3. The organic sub-blocks, $m_{i,1}$, i = 1,2,3,4, are considered as sinks/sources of the sub-blocks for inorganic matters, and the fluid cannot flow through organic matters. If a hydraulic fracture segment passes through a grid block, the matrix sub-blocks are assumed to be connected with this hydraulic fracture segment. The connection between the matrix and hydraulic fracture directly contributes a huge amount of gas to the wellbore, and hence it cannot be neglected in fractured reservoirs. The connection list of these blocks can be shown in Fig. 4b.

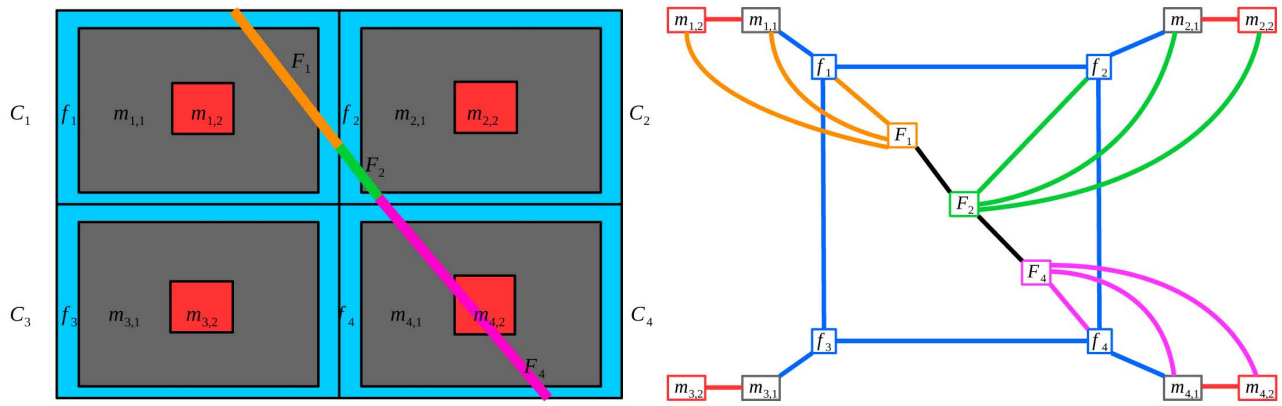

(a) A new model coupling the MINC and EDFM models

(b) Connection list of the new model

Figure 4—Example of the connection list for the new coupled model

Numerical Methods and Implementation

Our simulator is built on a parallel platform PRSI [21]. PRSI is written by the C language and MPI (Message Passing Interface), which is designed for large-scale reservoir simulation and provides a grid management module, a parallel input and output module, a linear solver module, a matrix/vector module and a well management module. In our previous work, we have implemented a parallel scalable black oil simulator [32] and a compositional simulator [33]. The Cartesian grids and corner point grids in Figs. 5a-5c are both supported by our simulator. The fully implicit method (FIM) [9] is used by our simulator, and in order to save the time of the solution of linear systems, the inexact Newton method [5] is utilized to automatically choose the required relative residual of each linear system. To enhance the efficiency of the solution process of linear systems and the parallel scalability, we extend the constrained pressure residual method [29, 3] in the research work [32, 23, 22, 10], and implement them in our simulator. To include the geomechanics

effects into reservoir simulation, a parallel geomechanics simulator using the finite element method on unstructured grids is developed in [24, 25] and has been iteratively coupled with our reservoir simulator.

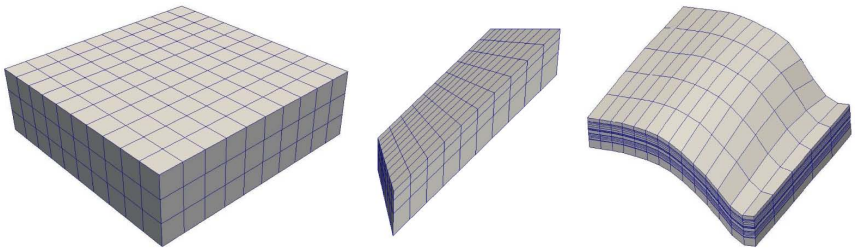

Figure 5—Grids

Numerical Experiments

Example 1

Water Flooding Case. We first consider a reservoir, which has $41 \times 41 \times 1$ *grid blocks. The dimension of each grid block is* (50*ft*, 50*ft*, 100*ft*). *One production well and one water injector are located at two corners of the reservoir. There are 4 large-scale fractures intersecting at the center of the reservoir. One of the large-scale fractures connects with the water injector. Details can be seen in Fig. 6 and Table 1.*

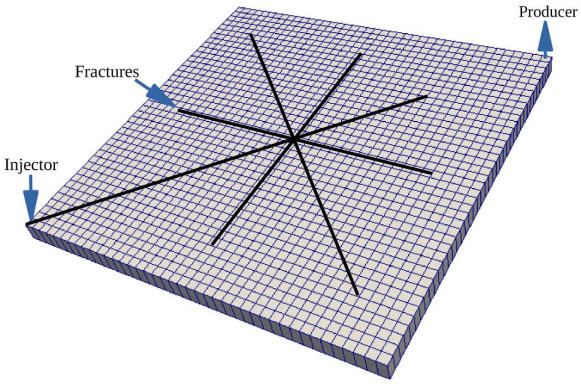

Figure 6—Water flooding case

Table 1—Parameters of the base case.

Parameter	Value	Unit
Grid blocks	$41 \times 41 \times 1$	
Block dimension (x,y,z)	(50,50,100)	ft
matrix porosity	0.03	
matrix permeability	(0.01,0.01,0.01)	md
matrix compressibility	3e-6	1/psi
Hydraulic fracture porosity	0.9	
Hydraulic fracture aperture	0.01	ft
Hydraulic fracture permeability	(5000,5000,2000)	md
Initial water saturation	0.12	
Initial oil saturation	0.88	
Simulation time	3650	day

The permeability of matrix is much lower than that of fractures, which means that the fractures are the main pathway for the fluid flow. Since one fracture connects with the water injector, most water is injected into this fracture, and water flows along with this fracture to other intersecting fractures. Consequently, the potential in the fractures becomes higher than that in the matrix. Driven by the difference of the potential, water flows from the fractures into the matrix. Because the permeability of the matrix is ultra-low, there is only a minor mass transfer between neighboring matrix blocks. From Fig. 7, the process of water flow is captured by our simulator.

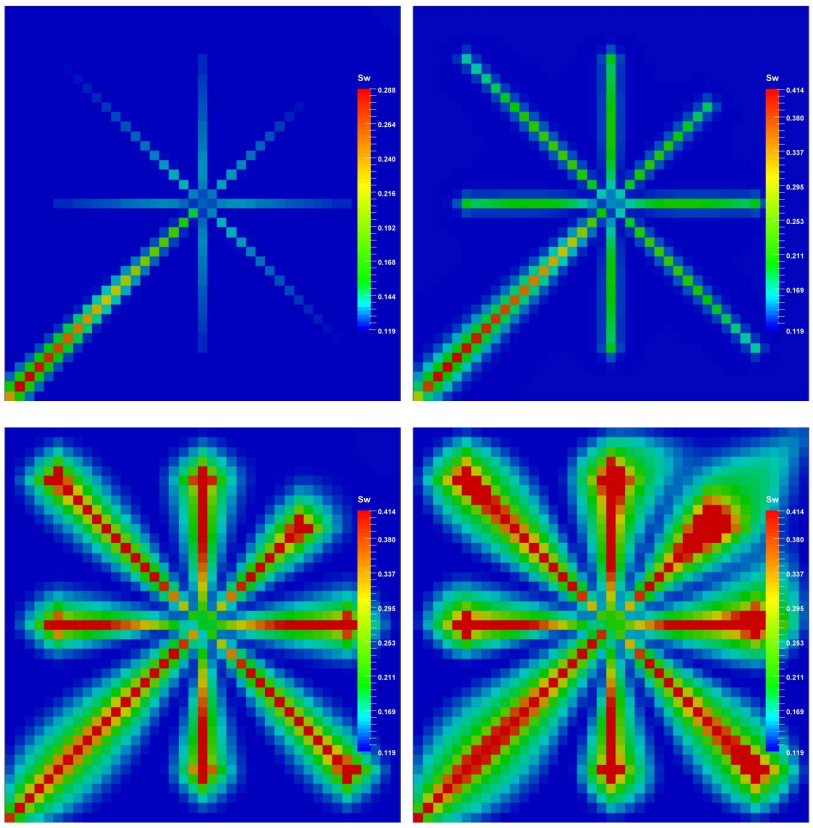

Figure 7—Water saturation change in the water flooding case

Example 2

Horizontal Well with Hydraulic Fractures Case. In the second case, we consider a reservoir, which has a horizontal well with four stages of hydraulic fracturing. Each of the main hydraulic fractures has secondary hydraulic fractures. The position of the well and hydraulic fractures is shown in Fig. 8. The details of this case can been seen in Table 2.

From Fig. 9, we can see that the pressure propagates along the directions of the dominant hydraulic fractures. In this case, we compare the production rate between with and without considering the secondary fractures. Since the secondary fractures are capable of making the responding region much larger, it is expected that more cumulative production can be obtained by the model with the secondary fractures. The cumulative production is plotted in Fig. 10.

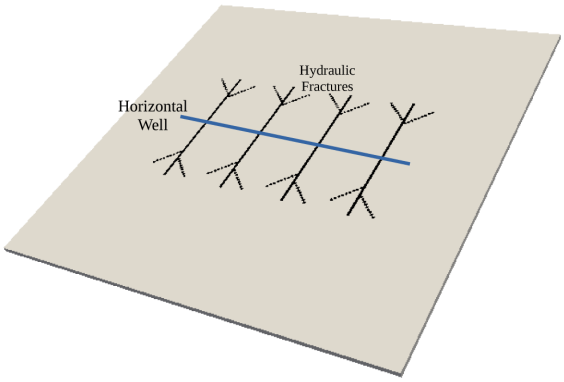

Figure 8—Horizontal well with hydraulic fractures case

Table 2—Parameters of the base case.

Parameter	Value	Unit
Grid blocks	165 × 165 × 1	
Block dimension (x,y,z)	(12.5,12.5,25)	ft
matrix porosity	0.03	
matrix permeability	(0.01,0.01,0.01)	md
matrix compressibility	3e-6	1/psi
Hydraulic fracture porosity	0.9	
Hydraulic fracture aperture	0.01	ft
Hydraulic fracture permeability	(5000,5000,2000)	md
Initial water saturation	0.12	
Initial oil saturation	0.88	
Simulation time	365	day

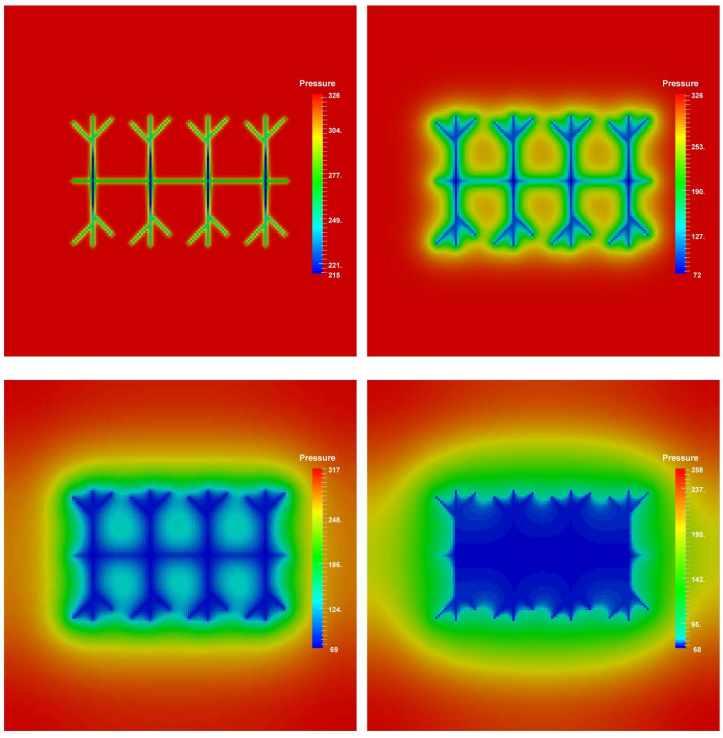

Figure 9—Pressure change for the horizontal well with hydraulic fractures case.

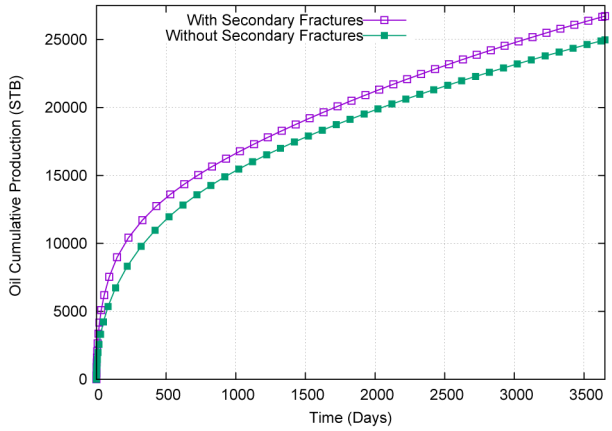

Figure 10—Cumulative production for the horizontal well with hydraulic fractures case.

Example 3

Complex Fracture Network Case. In the third case, the reservoir has one horizontal well and six stages of hydraulic fracturing. The hydraulic fractures and its secondary fractures form an irregular geometric pattern. The position of the six hydraulic fractures with the secondary fractures and the horizontal well are shown in Fig. 11. In this case, the natural fractures are assumed to pre-exist in the reservoir and are represented by the MINC model. The geomechanics effects, gas adsorption/desorption and non-Darcy flow mechanisms are also considered. The details of this case can be seen in Table 3.

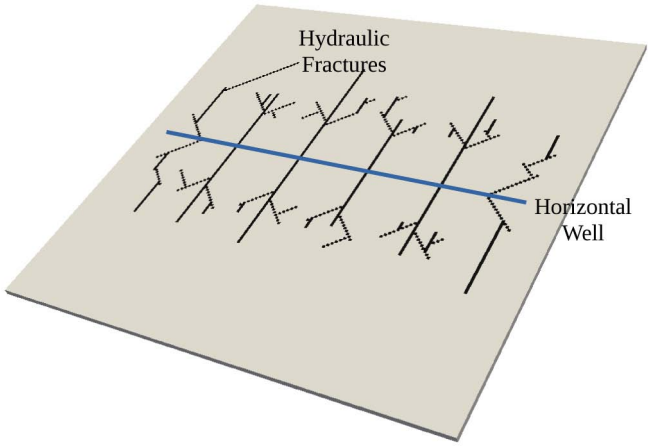

Figure 11—Complex fracture network case

Table 3—Parameters of the base case.

Parameter	Value	Unit
Grid blocks	165 × 165 × 1	
Block dimension (x,y,z)	(12.5,12.5,25)	ft
Organic matter volume percentage	20%	
Organic matter porosity	0.4	
Organic matter permeability	(1e-4,1e-4,1e-4)	md
Organic matter compressibility	1e-7	1/psi
Organic material density	400	lbm/ft^3
Inorganic material volume percentage	80%	
Inorganic material porosity	0.2	
Inorganic material permeability	(1e-3,1e-3,5e-4)	md
Inorganic material compressibility	1e-7	1/psi
Hydraulic fracture porosity	0.9	
Hydraulic fracture aperture	0.01	ft
Hydraulic fracture permeability	(5000,5000,2000)	md
Hydraulic fracture compressibility	4e-5	1/psi
Natural fracture spacing	(10,10,10)	ft
Natural fracture aperture	0.001	ft
Natural fracture permeability	(125,125,125)	ft
Natural fracture compressibility	4e-4	1/psi
Natural fracture shape factor	GK	
Biot coefficient	1.0	
Poisson's ratio	0.33	
Langmuir volume	1.8e-5	ft^3/lbm
Langmuir pressure	10000	psi
Temperature	157.73	F
Initial natural fracture S_w	0.11	
Initial natural fracture S_g	0.89	
Initial hydraulic fracture S_w	0.22	
Initial hydraulic fracture S_g	0.78	
Initial matrix S_w	0.18	
Initial matrix S_g	0.82	
Simulation time	365	day

From Fig. 12, as we can see, the pressure of the matrix blocks along with the hydraulic fractures has the most dramatic decrease.

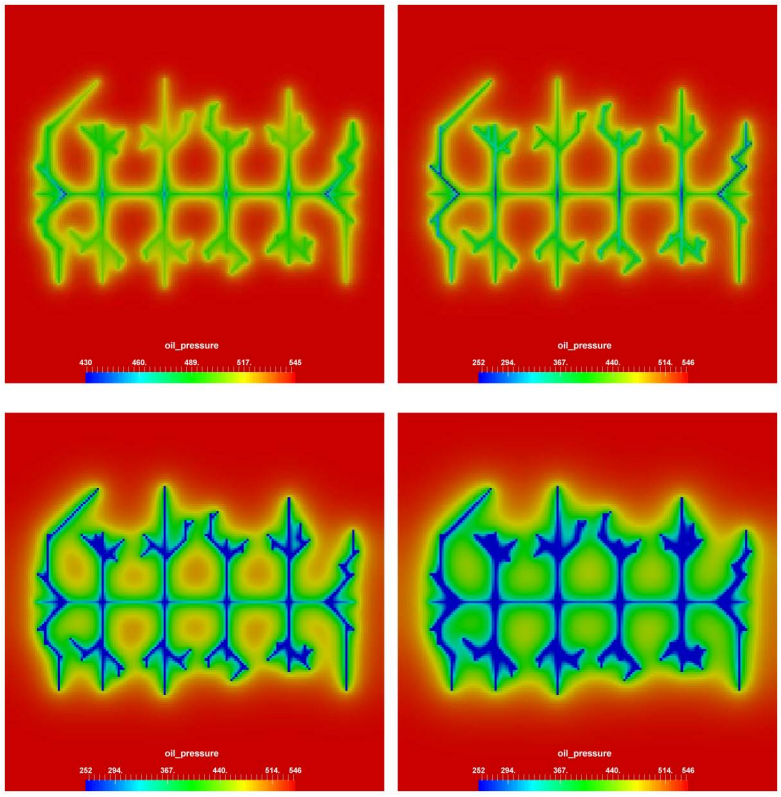

Figure 12—Pressure change in the complex fracture network case.

Fig. 13 shows the gas saturation profile in the natural fractures. At the early time of production, since the permeability of the natural fractures is much larger than that of the matrix, most of the produced gas comes from the pathway of the natural fracture and hydraulic fracture. As a result, the gas saturation along with the hydraulic fractures is the smallest. The reservoir pressure drops during the process of production, and the reduction of the permeability of the natural fractures appears. The permeability of the natural fractures approaches or even is smaller than that of the matrix, and then the matrix medium becomes the main pathway for the fluid to flow. The gas from the matrix flows not only to the hydraulic fractures but also to the natural fractures. Consequently, the gas saturation in the natural fractures on the blocks along with the hydraulic fractures is higher than in the neighbors; see the right bottom figure of Fig. 13. If the geomechanics effects and the new coupled model developed in the section are not employed, this phenomenon will not be captured.

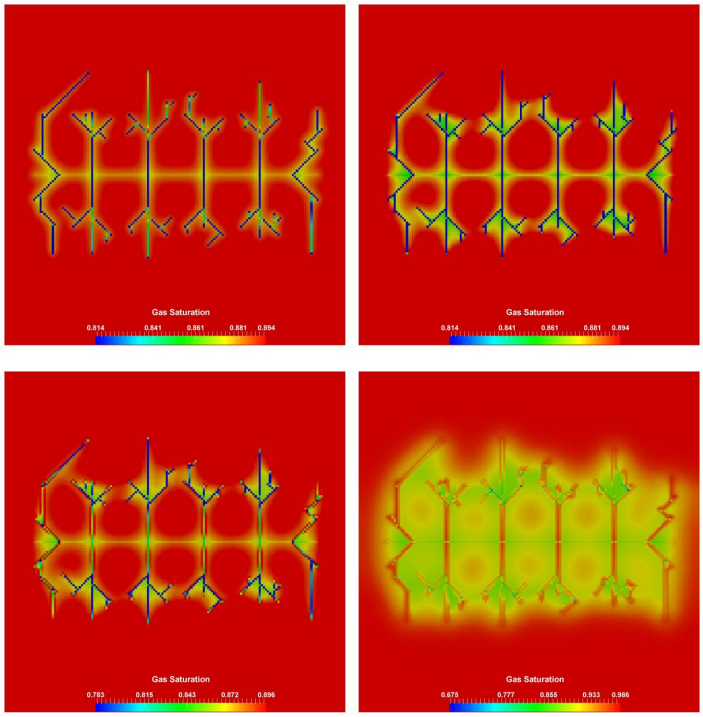

Figure 13—Gas saturation change for the complex fracture network case.

Conclusions

In this paper, we have developed a parallel simulator for fractured unconventional reservoirs. A MINC model and an embedded discrete fracture model as well as a coupled model are adopted by the simulator to handle fractures with different scales. The gas adsorption/desorption, non-Darch flow and geomechanics effects are taken into consideration by this simulator. There are no restrictions on the geometry of fractures, and the geometry can be configured by the users. From the simulation results, we can see that our simulator is capable of modeling unconventional gas and oil reservoirs with multi-scale fractures. Reasonable physical phenomena and accurate production prediction are both obtained by our simulator.

Acknowledgement

The support of the Department of Chemical and Petroleum Engineering, University of Calgary and Reservoir Simulation Group is gratefully acknowledged. The research is partly supported by NSERC/AIEES/Foundation CMG, AITF (iCore), IBM Thomas J. Watson Research Center, and the Frank and Sarah Meyer FCMG Collaboration Centre for Visualization and Simulation. The research is also enabled in part by support provided by WestGrid (www.westgrid.ca), SciNet (www.scinethpc.ca) and Compute Canada Calcul Canada (www.computecanada.ca).

References

1. Raymond J Ambrose, Robert C Hartman, Mery Diaz-Campos, I Yucel Akkutlu, Carl H Sondergeld, et al. Shale gas-in-place calculations part i: new pore-scale considerations. *SPE Journal*, **17**(01):219-229,2012.
2. G Alda Behie and PA Forsyth, Jr. Incomplete factorization methods for fully implicit simulation of enhanced oil recovery. *SIAM Journal on Scientific and Statistical Computing*, **5**(3):543-561,1984.

3. Hui Cao, Hamdi A Tchelepi, John Richard Wallis, Hrant E Yardumian, et al. Parallel scalable unstructured cpr-type linear solver for reservoir simulation. In SPE Annual Technical Conference and Exhibition. Society of Petroleum Engineers, 2005.
4. Dong Chen, Zhejun Pan, and Zhihui Ye. Dependence of gas shale fracture permeability on effective stress and reservoir pressure: model match and insights. *Fuel*, **139**:383-392,2015.
5. Teng Chen, Nicholas Gewecke, Zhen Li, Andrea Rubiano, Robert Shuttleworth, Bo Yang, and Xinghui Zhong. Fast computational methods for reservoir flow models. *IMA Preprint Series*, 2286, 2009.
6. Zhangxin Chen. Bdm mixed methods for a nonlinear elliptic problem. *Journal of computational and applied mathematics*, **53**(2): 207-223, 1994.
7. Zhangxin Chen and Jim Douglas Jr. Approximation of coefficients in hybrid and mixed methods for nonlinear parabolic problems. *Mat. Aplic. Comp*, **10**:137-160,1991.
8. Zhangxin Chen, Magne Espedal, and Richard E Ewing. Continuous-time finite element analysis of multiphase flow in groundwater hydrology. *Applications of Mathematics*, **40**(3):203-226,1995.
9. Zhangxin Chen, Guanren Huan, and Yuanle Ma. Computational methods for multiphase flows in porous media, volume **2**. *Siam*, 2006.
10. Tao Cui, Kun Wang, Hui Liu, Jia Luo, Zhangxin Chen, et al. Efficient and scalable methods for dual-porosity/permeability models in fractured reservoir simulations. In SPE Asia Pacific Oil & Gas Conference and Exhibition. Society of Petroleum Engineers, 2016.
11. A. H. Dogru, H. A. Sunaidi, L. S. Fung, W. A. Habiballah, N. Al-Zamel, and K. G. Li. A parallel reservoir simulator for large-scale reservoir simulation. *SPE Reservoir Evaluation & Engineering*, **5**(1): 11-23,2002.
12. Ali H. Dogru, Larry Siu Kuen Fung, Usuf Middya, Tareq Al-Shaalan, and Jorge Alberto Pita. A next-generation parallel reservoir simulator for giant reservoirs. In SPE/EAGE Reservoir Characterization & Simulation Conference, 2009.
13. D.G. Hill and C.R. Nelson. Gas productive fractured shales an overview and update. *Gas TIPS*, **6**(2):4-13,2000.
14. Xiaozhe Hu, Wei Liu, Guan Qin, Jinchao Xu, Zhensong Zhang, et al. Development of a fast auxiliary subspace pre-conditioner for numerical reservoir simulators. In SPE Reservoir Characterisation and Simulation Conference and Exhibition. Society of Petroleum Engineers, 2011.
15. Farzam Javadpour. Nanopores and apparent permeability of gas flow in mudrocks (shales and siltstone). *Journal of Canadian Petroleum Technology*, **48**(08):16-21,2009.
16. Jiamin Jiang and Rami M Younis. A multimechanistic multicontinuum model for simulating shale gas reservoir with complex fractured system. *Fuel*, **161**:333-344,2015.
17. Jiamin Jiang and Rami M Younis. Numerical study of complex fracture geometries for unconventional gas reservoirs using a discrete fracture-matrix model. *Journal of Natural Gas Science and Engineering*, **26**:1174-1186,2015.
18. Jiamin Jiang, Rami Younis, et al. Hybrid coupled discrete-fracture/matrix and multicontinuum models for unconventional-reservoir simulation. *SPE Journal*, 2015.
19. Liyong Li, Seong H Lee, et al. Efficient field-scale simulation of black oil in a naturally fractured reservoir through discrete fracture networks and homogenized media. *SPE Reservoir Evaluation & Engineering*, **11**(04):750-758,2008.
20. Xiang Li, Dongxiao Zhang, and Sanbai Li. A multi-continuum multiple flow mechanism simulator for unconventional oil and gas recovery. *Journal of Natural Gas Science and Engineering*, **26**:652-669,2015.

21. Hui Liu, Kun Wang, Zhangxin Chen, Kirk E Jordan, Jia Luo, Hui Deng, et al. A parallel framework for reservoir simulators on distributed-memory supercomputers. In SPE/IATMI Asia Pacific Oil & Gas Conference and Exhibition. Society of Petroleum Engineers, 2015.
22. Hui Liu, Kun Wang, Zhangxin Chen, Kirk E Jordan, et al. Efficient multi-stage preconditioners for highly heterogeneous reservoir simulations on parallel distributed systems. In SPE Reservoir Simulation Symposium. Society of Petroleum Engineers, 2015.
23. Hui Liu, Kun Wang, and Zhangxin Chen. A family of constrained pressure residual preconditioners for parallel reservoir simulations. *Numerical Linear Algebra with Applications*, **23**(1):120-146,2016.
24. Jia Luo, Zhangxin Chen, Kun Wang, Hui Deng, Hui Liu, et al. An efficient and parallel scalable geomechanics simulator for reservoir simulation. In SPE/IATMI Asia Pacific Oil & Gas Conference and Exhibition. Society of Petroleum Engineers, 2015.
25. Jia Luo, Kun Wang, Hui Liu, and Zhangxin Chen. Coupled geomechanics and fluid flow modeling in naturally fractured reservoirs. In Low Permeability Symposium. Society of Petroleum Engineers, 2016.
26. Ali Moinfar, Abdoljalil Varavei, Kamy Sepehrnoori, Russell T Johns, et al. Development of a coupled dual continuum and discrete fracture model for the simulation of unconventional reservoirs. In SPE Reservoir Simulation Symposium. Society of Petroleum Engineers, 2013.
27. Karsten Pruess et al. A practical method for modeling fluid and heat flow in fractured porous media. *Society of Petroleum Engineers Journal*, **25**(01):14-26,1985.
28. Yousef Saad. Krylov subspace methods for solving large unsymmetric linear systems. *Mathematics of computation*, **37**(155): 105-126,1981.
29. JR Wallis, RP Kendall, TE Little, et al. Constrained residual acceleration of conjugate residual methods. In SPE Reservoir Simulation Symposium. Society of Petroleum Engineers, 1985.
30. JR Wallis et al. Incomplete gaussian elimination as a preconditioning for generalized conjugate gradient acceleration. In SPE Reservoir Simulation Symposium. Society of Petroleum Engineers, 1983.
31. Jing Wang, Haishan Luo, Huiqing Liu, Fei Cao, Zhitao Li, Kamy Sepehrnoori, et al. An integrative model to simulate gas transport and production coupled with gas adsorption, non-darcy flow, surface diffusion, and stress dependence in organic-shale reservoirs. *SPE Journal*, 2016.
32. Kun Wang, Hui Liu, and Zhangxin Chen. A scalable parallel black oil simulator on distributed memory parallel computers. *Journal of Computational Physics*, **301**:19-34,2015.
33. Kun Wang, Hui Liu, Jia Luo, and Zhangxin Chen. A multi-continuum multi-phase parallel simulator for large-scale conventional and unconventional reservoirs. *Journal of Natural Gas Science and Engineering*, **33**:483-496,2016.
34. JE Warren, P Jj Root, et al. The behavior of naturally fractured reservoirs. Society of Petroleum Engineers Journal, **3**(03):245-255, 1963.
35. Keliu Wu, Zhangxin Chen, and Xiangfang Li. Real gas transport through nanopores of varying cross-section type and shape in shale gas reservoirs. *Chemical Engineering Journal*, **281**:813-825,2015.
36. Yu-Shu Wu, Karsten Pruess, et al. A multiple-porosity method for simulation of naturally fractured petroleum reservoirs. *SPE Reservoir Engineering*, **3**(01):327-336,1988.
37. Rui-han Zhang, Lie-hui Zhang, Rui-he Wang, Yu-long Zhao, and Rui Huang. Simulation of a multistage fractured horizontal well with finite conductivity in composite shale gas reservoir through finite-element method. *Energy & Fuels*, **30**(11):9036-9049,2016.